

Pinhole junctions in d-wave superconductors

Mikael Fogelström^{a,b}, Sungkit Yip^{a *} and Juhani Kurkijärvi^{a,b}

^a*Department of Physics & Astronomy, Northwestern University, Evanston, Illinois 60208, U. S. A.*

^b*Department of Physics, Åbo Akademi, Porthansgatan 3, 20500 Åbo, Finland*

(Accepted for publication in Physica C)

We present a self consistent treatment of pinhole junctions in $d_{x^2-y^2}$ superconductors. The current-phase relation $j_s(\chi)$ is studied at different temperatures and at different angles α between the crystal \hat{a} -axis and the junction (surface) normal. We show that the critical current of a junction can be reduced by pair-breaking effects at the separation. We also study the Josephson energy of a pinhole as a function of the phase difference across the junction. In particular are mapped the positions of the energy minima χ_{min} at different temperatures as functions of (α_L, α_R) , the crystal orientations of the left and right superconductors. With decreasing temperature there is an increasing range of crystal orientations where χ_{min} varies continuously from 0 to π .

PACS numbers: 74.50.+r, 74.72.-h

keywords: superconducting junctions, unconventional pairing

I. INTRODUCTION

Recent experiments and their interpretations have strongly argued in favor of an order parameter of B_{1g} ($d_{x^2-y^2}$) symmetry in the oxide superconductors (see e.g. reviews^{1,2}). Part of the evidence comes from bulk and transport properties (see¹). Other relevant data involve Josephson junctions which probe the order parameter at surfaces. In these latter experiments, the phase of the order parameter is involved, and "interference" experiments can be carried out.

It will be important below to realize that interference experiments fall into two categories. In the first one measures the critical current of a two junction loop as a function of the magnetic flux threading the ring and records the positions of the current maxima³⁻⁸. The second type consists of mapping the phase differences at the Josephson energy minima⁹⁻¹³.

Josephson junctions in s-wave superconductors have been well explored. Here we distinguish between "tunnel" junctions on the one hand and "weak-links" on the other. We shall follow¹⁴ and classify junctions on the basis of their *normal-state* conductivities. In a tunnel junction normal electrons face a reasonably high potential barrier whereas in a weak-link junction they do not.

Even in s-wave superconductors, tunnel junctions and weak links behave in different fashions. We compare weak-link junctions with tunnel junctions in unconventional superconductors picking the pinhole as the representative of the former. The differences arise from two sources: Firstly, the current-phase relation of a tunnel junction is sinusoidal. The minima/maxima of the Josephson energy therefore lie at a phase difference equal to zero or π (provided the order parameter does not break time-reversal symmetry¹⁵). In a weak link, the current-phase relationship is not sinusoidal in general^{15,16}, and the minima/maxima will not lie at zero or π . Secondly, in weak links the current carrying processes sample a wider angular range of momentum than in tunnel junctions. With different crystal orientations on the two sides of a junction, varying the angle of the junction with respect to the crystals, one observes quite different behaviors of the positions of the energy minima and critical current in pinholes and in tunnel junctions.

Nevertheless, "weak-links", (especially our pinhole) and tunnel junctions are the opposite ends of a continuum. Imagining a weak potential barrier in the link and increasing its strength should take one smoothly from the pinhole to the tunnel junction.

Josephson junctions are probes of surfaces. Near a surface, an unconventional order parameter must be strongly affected^{17,18}. We therefore also investigate the effect of surface pair breaking on our weak links and tunnel junctions.

Most of the discussions on high- T_c junctions in the literature ignore the difference between weak links and tunnel junctions (and the effects of surface pair-breaking). In the sequel it is argued in some detail that a number of puzzling reports in the literature may have a natural explanation if one keeps track of these effects. One should be very careful when drawing conclusions on the order parameter type of a high T_c superconductor on the basis of measurements of various Josephson-related effects. All available models and their variants should be checked out for competing interpretations.

*corresponding author, fax: +1 847-491-9982, e-mail: yip@snowmass.phys.nwu.edu

In Section 2 we discuss the self-consistently computed junctions, first pinholes (weak links) and then tunnel junctions in Section 3. Section 4 is about the non self-consistent junctions, i.e. those treated analytically assuming constant order parameters up to the separation where the junction sits. Section 4 ends with the Subsection 4.1 which compares the self-consistent and non self-consistent models introduced in the previous Sections. Section 5 is on critical currents and phase differences where the Josephson energy reaches its minima. The final Section 6 is on the conclusions we suggest from experiments. The ultimate Section 6.3 is a critical analysis of the plausibility of our models as describing real junctions.¹

II. THE PINHOLE JUNCTION

The pinhole junction is a small opening in an interface separating two superconductors (see Figure 1), small both in length and in width on the scale of the coherence length ξ_0 . Being so tiny, the opening perturbs little the order parameter which may be calculated ignoring the pinhole. A phase difference χ over the junction is introduced multiplying the self-consistent order parameters on the two sides with the factors $\exp(\pm i\chi/2)$. The phase is taken to hop discontinuously at the partition. The pinhole junction was first introduced in s-wave superconductors²⁰ and has also been considered as a model of a weak link in superfluid ^3He ^{21,22}.

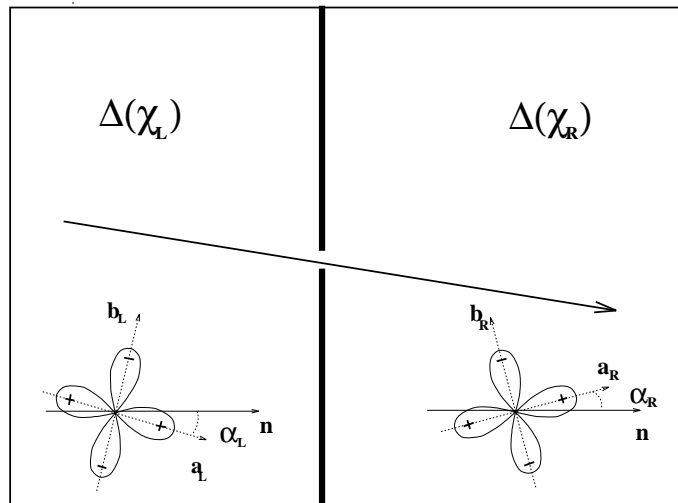


FIG. 1. Sketch of a pinhole. The opening is small on the scale of coherence length. Most trajectories are reflected at the interface, and only those hitting the hole are transmitted.

A. The self-consistent pinhole

Surfaces have a pair-breaking effect on a superconductor whose order parameter depends on the direction $\hat{\mathbf{p}}$ of propagation of a quasiparticle, and we need to take into account the quasiparticle scattering at the wall. Models for walls have been studied in ^3He (see, for instance,²³ and²⁴) and recently also in d-wave superconductors (¹⁸,²⁵ and²⁶). We chose the specular surface, attractive in its simplicity. It has been studied by¹⁸. The Green's function $\hat{g}(\hat{\mathbf{p}}, \mathbf{R}; \epsilon_n)$ in the specular model is taken to be continuous at the surface along pairs of trajectories $(\hat{\mathbf{p}}_{in}, \hat{\mathbf{p}}_{out})$ connected as

$$\hat{\mathbf{p}}_{out} = \hat{\mathbf{p}}_{in} - 2\hat{\mathbf{n}}(\hat{\mathbf{n}} \cdot \hat{\mathbf{p}}_{in}), \quad (1)$$

$\hat{\mathbf{n}}$ being the surface normal.

With the boundary conditions set, the procedure of getting at the order parameter consists of iterating the Eilenberger equation

¹We shall only consider planar interfaces. Some recent papers (e.g.¹⁹ and references therein) have suggested that it may be important to include the effects of facets in understanding the properties of some grain boundaries. If this is so, then we cannot directly apply our results to these grain boundaries; instead they can only serve as inputs when considering the facets.

$$[i\epsilon_n \hat{\tau}_3 - \hat{\Delta}(\hat{\mathbf{p}}, \mathbf{R}), \hat{g}(\hat{\mathbf{p}}, \mathbf{R}; \epsilon_n)] + i\mathbf{v}_f \cdot \nabla_{\mathbf{R}} \hat{g}(\hat{\mathbf{p}}, \mathbf{R}; \epsilon_n) = 0 \quad (2)$$

for the propagator, where \mathbf{v}_f is the Fermi velocity and $\hat{\mathbf{p}}$ the direction of momentum at the Fermi surface, together with the gap equation for the order parameter

$$\Delta(\hat{\mathbf{p}}, \mathbf{R}) = \pi T \sum_{\epsilon_n} \int \frac{d\Omega_{\hat{\mathbf{p}}'}}{4\pi} V(\hat{\mathbf{p}}, \hat{\mathbf{p}}') \frac{1}{2} \text{Tr}\{(\hat{\tau}_1 - i\hat{\tau}_2) \hat{g}(\hat{\mathbf{p}}', \mathbf{R}; \epsilon_n)\} \quad (3)$$

till self consistency. As indicated by the carets, the propagator \hat{g} and the order parameter $\hat{\Delta}$ are matrices in the particle-hole space². The order parameter is conveniently parameterized in terms of a real part Δ_2 and an imaginary part Δ_1 as $\hat{\Delta} = i(\Delta_1 \hat{\tau}_1 + \Delta_2 \hat{\tau}_2)$. Only interested in an equilibrium property, we can use the Matsubara formalism at the Matsubara frequencies $\epsilon_n = \pi T(2n + 1)$.

The pairing interaction $V(\hat{\mathbf{p}}, \hat{\mathbf{p}}')$ in equation (3) determines the symmetry of the order parameter. $V(\hat{\mathbf{p}}, \hat{\mathbf{p}}')$ can be separated into a sum of allowed pairing channels. The strength of a particular channel X depends on the coupling parameter $\frac{1}{V(X)}$ which can be eliminated in favor of the transition temperature $T_c(X)$ in the channel with the aid of the well-known BCS-relation

$$\frac{1}{V(X)} = \ln \frac{T}{T_c(X)} + \sum_{n \geq 0}^{n_c} \frac{1}{n + \frac{1}{2}} \quad (4)$$

where n_c is a cutoff. In this work, the dominant pairing channel is always chosen as having an order parameter of B_{1g} symmetry. Buchholtz et al¹⁸ have shown that for equal $V(X)$ in the subdominant channels, B_{2g} has the strongest effect on the properties of a smooth surface. Thus we follow¹⁸ and study a superconductor with a $d_{x^2-y^2}$ or B_{1g} order parameter in the bulk and allow an admixture of a d_{xy} or B_{2g} component close to the surface. The degree of mixing is controlled by the ratio of the transition temperatures of the two representations. This ratio is a parameter of the present calculation. The pairing interaction is

$$V(\hat{\mathbf{p}}, \hat{\mathbf{p}}') = 2V_{B_{1g}} \cos 2\phi \cos 2\phi' + 2V_{B_{2g}} \sin 2\phi \sin 2\phi'. \quad (5)$$

We refer to¹⁸ for a full account of the behavior of the order parameter at a surface and only briefly summarize the principal effects here. Imagine a superconducting crystal with a $d_{x^2-y^2}$ order parameter cut with a surface whose normal is $\hat{\mathbf{n}}$. In a thin film sample, $\hat{\mathbf{n}}$ would lie normal to the junction in the plane of the film. The d-wave order parameter is reduced when the crystal is rotated relative the surface (junction) normal $\hat{\mathbf{n}}$ to a position determined by the angle α between the crystal \hat{a} -axis and the normal $\hat{\mathbf{n}}$ (see Fig. 1)³. The order parameter is unaffected by the presence of the surface (=cut) if the crystal has its \hat{a} or \hat{b} -axis parallel to $\hat{\mathbf{n}}$. It is maximally reduced when α is equal to $\frac{\pi}{4} + n\frac{\pi}{2}$, n being an integer. In the latter case, the order parameter vanishes identically at the wall. If the ratio of transition temperatures is chosen larger than zero, a B_{2g} component may develop in the vicinity of the wall. A special case is at α close to $\frac{\pi}{4}$ at temperatures $T/T_c(B_{1g}) \leq T_c(B_{2g})/T_c(B_{1g})$ where the composite order parameter is found to break time-reversal symmetry^{25,27}.

There is, however, a problem associated with mixing two representations as described above. On the basis of the boundary condition $\hat{g}(\hat{\mathbf{p}}_{in}, \mathbf{0}; \epsilon_n) = \hat{g}(\hat{\mathbf{p}}_{out}, \mathbf{0}; \epsilon_n)$, eq (3) and the general symmetries of the propagator⁴ one can show that (see also²⁹), for $T_c(B_{2g})$ different from zero, the ratio of the two order parameter components at the wall is⁵

$$\frac{\Delta_{B_{2g}}(0)}{\Delta_{B_{1g}}(0)} = -\frac{V_{B_{2g}}}{V_{B_{1g}}} \tan 2\alpha. \quad (6)$$

Numerically this becomes

² The propagator is decomposed as $\hat{g} = \sum_{i=1}^3 g_i \hat{\tau}_i$, $\hat{\tau}_i$ being the Pauli matrices.

³We take the $d_{x^2-y^2}$ order parameter as having its positive lobe along the the crystal \hat{a} axis and its negative lobe along the \hat{b} -axis.

⁴For symmetries obeyed by propagators and self energies, see²⁸.

⁵It seems that eq. 6 must reflect itself in the boundary condition that should be used in a phenomenological Ginzburg-Landau theory. It is unclear whether this has been taken into account properly in the literature (e.g.³⁰)

$$\frac{\Delta_{B_{2g}}(0)}{\Delta_{B_{1g}}(0)} = -\tan 2\alpha \left(1 + \frac{\ln \frac{T_c(B_{1g})}{T_c(B_{2g})}}{\ln \frac{T}{T_c(B_{1g})} + \sum_{n \geq 0}^{n_c} \frac{1}{n + \frac{1}{2}}} \right) \quad (7)$$

i.e. the ratio is cutoff dependent. We must keep track of the the cutoff as soon as the T_c -ratio is non-zero. The results given below are all at the cutoff $n_c(T/T_c)$ chosen equal to the integer part of $16T_c/T$.

With the order parameter determined self-consistently, we can calculate the current-phase relation across a junction. For this we need the Green's function at the orifice. The propagator is computed along trajectories through the orifice (see Figure 1). The boundary condition is boundedness far away on both sides of the interface. At the orifice, the propagator is matched for continuity. An alternative route is the multiplication trick³¹. This slight of hand takes advantage of exploding solutions along trajectories towards the junction. The matrix commutator of each pair of diverging solutions on the same trajectory at the pinhole (in fact an exploding solution and a decaying solution if viewed as propagating in the same direction) delivers the physical propagator in the orifice. The current density for a given phase difference χ is calculated from the propagator in the orifice (at $\mathbf{R} = 0$) by

$$j_s(\chi, T) = 2eN_f v_f T \sum_{\epsilon_n} \int_{>} \frac{d\phi}{2\pi} \cos \phi \text{Tr}_2[\hat{\tau}_3 \hat{g}_\chi(\hat{\mathbf{p}}, 0; \epsilon_n)]. \quad (8)$$

Here N_f is the density of states at the Fermi surface, and $>$ on the integral means that only the half sphere $\hat{\mathbf{n}} \cdot \hat{\mathbf{p}} > 0$ of directions are included. In general the Fermi velocity and the density of states depend on the position on the Fermi surface $\hat{\mathbf{p}}$. We assume a circular Fermi surface, for which the Fermi velocity is $\mathbf{v}_f = v_f \hat{\mathbf{p}}$. This assumption is not an unreasonable simplification. Buchholtz *et al.*¹⁸ compared calculations of the order parameter and the surface density of states using a cylindrical Fermi surface with the same calculations using a Fermi surface calculated from a tight-binding model³². They found very small differences between the two models.

The phase dependent part of the Josephson energy density can be calculated from the current-phase relation as

$$E_s(\chi, T) = E_s(\chi_0, T) + \frac{\hbar}{2e} \int_{\chi_0}^{\chi} d\chi' j_s(\chi', T). \quad (9)$$

Equation (9) is valid for all the junctions discussed in the present article.

III. THE TUNNEL JUNCTION

As announced in the introduction, we wish to compare weak link junctions with tunnel junctions. A tunneling barrier is characterized by its transparency $D(\phi)$. Self consistent or not, the transparency of the junction may depend on the direction of the incident momentum (ϕ being the angle $\hat{\mathbf{p}}$ makes with the surface normal). We have chosen a transmission coefficient proportional to $\exp(-8 \sin^2 \phi)$, i.e. peaked in the forward direction. This model transmission is used though out this paper with one exception. In the initial discussion in Section V B the transmission coefficient is chosen as all peaked along the junction normal. This we refer to as the forward (backward) tunneling limit.

A. The self-consistent tunnel junction

The self-consistent order-parameter calculation of Section II A works here as well since the tunneling potential barrier is high enough to perturb the order parameters on the two sides only little. For calculating the tunneling current we take the expression of³³

$$j_s(\chi, T) = \frac{2eN_f v_f}{\pi} T \sum_{\epsilon_n} \int_{>} \frac{d\phi}{2\pi} D(\phi) \cos \phi [g_2^L(-\chi) g_1^R(\chi) - g_2^R(\chi) g_1^L(-\chi)] \quad (10)$$

where $g_{1,2}^{R,L}$ are the anomalous part of the propagator at the tunneling barrier (in our case at the surface) in either superconductor.

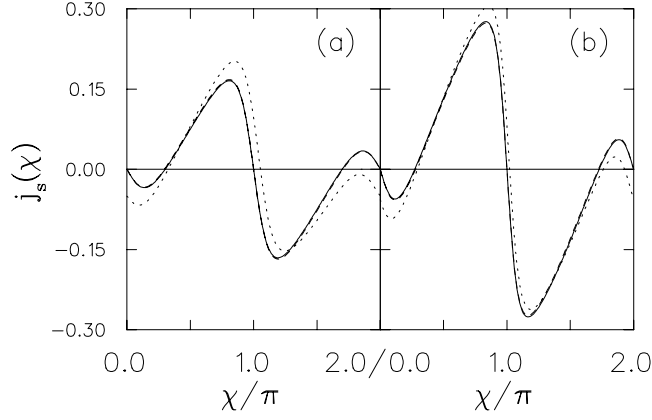


FIG. 2. Current-phase relation of a weak link with $\alpha_L = 9\pi/40$ and $\alpha_R = \pi/40$ and temperature $0.1 T_c(B_{1g})$. (a) self-consistent current relations for three different T_c -ratios: 0 (solid line), 10^{-3} (dashed line) and 10^{-1} (dotted line). (b) mimicking the self-consistent current-phase relation via a mixture of B_{1g} and B_{2g} . The choices are: Pure B_{1g} order parameters in both superconductors (solid line), $\Delta^{R,L}(\phi) = \Delta_{B_{1g}} - 0.05\Delta_{B_{2g}}(\phi)$ (dashed line) and $\Delta^L(\phi) = \Delta_{B_{1g}}(\phi)$ and $\Delta^R(\phi) = \Delta_{B_{1g}}(\phi) - 0.05i\Delta_{B_{2g}}(\phi)$ (dotted line). (a) and (b) the dotted lines: states breaking time-reversal symmetry.

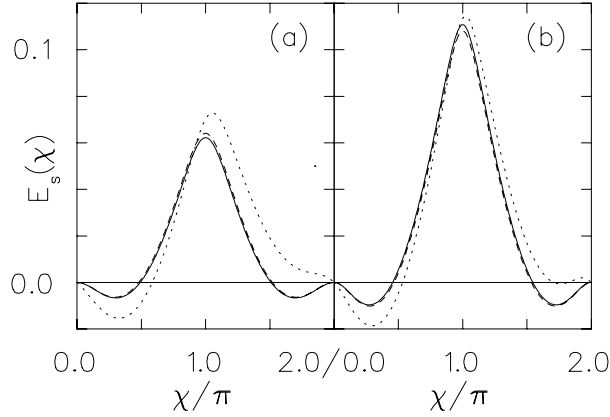


FIG. 3. Energy-phase relation for the same junction as in figure 2. Lines as in Fig. 2

IV. NON SELF-CONSISTENT JUNCTIONS

Most of the time we investigate the junctions with the order parameter self-consistently calculated. As a point of comparison, we consider the case of a constant order parameter up to the surface^{34,15,16}. This non self-consistent calculation can usually be done analytically. Comparing with the self consistent calculations we get a measure on the effects of surface pair breaking on the current-phase and the energy-phase relations.

Consider a junction, weak link or tunnel junction, with order parameters left unaffected by scattering at the wall or the junction surface. Assuming tetragonal crystal symmetry, the bulk-gap function in d-wave superconductors is

$$\Delta_{B_{1g}}(\hat{\mathbf{p}}) = \Delta \cos 2(\phi - \alpha) \quad (11)$$

for order parameters of $d_{x^2-y^2}$ or B_{1g} symmetry and

$$\Delta_{B_{2g}}(\hat{\mathbf{p}}) = \Delta \sin 2(\phi - \alpha) \quad (12)$$

for order parameter of d_{xy} or B_{2g} symmetry. Δ is the temperature dependent maximal amplitude of the gap and ϕ the angle $\hat{\mathbf{p}}$ makes with respect to the junction normal $\hat{\mathbf{n}}$.

The expressions for the current through the junctions are calculated inserting the bulk propagators into equations (8) and (10). The weak link current is given by³⁴, and the tunnel-junction current is basically the well known Ambegaokar-Baratoff formula³⁵.

A. Self-consistent pinhole versus non self-consistent pinhole

We calculate and compare the current-phase (Fig. 2) and the energy-phase relations (Fig. 3) for a self consistent (a) and a non-self-consistent (b) weak link at different T_c -ratios at $T = 0.1T_c$. The crystal orientations are chosen as $\alpha_L = 9\pi/40$ and $\alpha_R = \pi/40$. We see that even with a pure B_{1g} order parameter, the very similar current-phase relationships differ significantly from the sinusoidal form. The energy minima occur at some χ , neither equal to 0 nor π . If we admit, in a self-consistent fashion, a small B_{2g} -order parameter, the critical current increases a little but the energy minima are not shifted in position. When, on the other hand, the T_c -ratio is set equal to the temperature (dotted line in (a) and (b)), the system is just on the edge of the area in the parameter space where the superconducting state will spontaneously break time-reversal symmetry near the surface. There the current-phase relation no longer obeys the symmetry $j_s(\chi) = -j_s(-\chi)$ and the critical current is increased.

Turning to the equally very similar energy-phase relations, we see that the symmetry of the time-reversal invariant relation has been lost at the edge of the instability against a time-reversal symmetry breaking state (TRSB). This applies also to the mimicked state in the non self-consistent case (dotted line in (b)). The junction can in fact be in two distinct states (with different order parameters). The second state has $E_s(\chi) \rightarrow E_s(2\pi - \chi)$ (not shown).

An overall conclusion is that the principal effect of pair braking on a surface reflects itself as a simple reduction of the critical current.

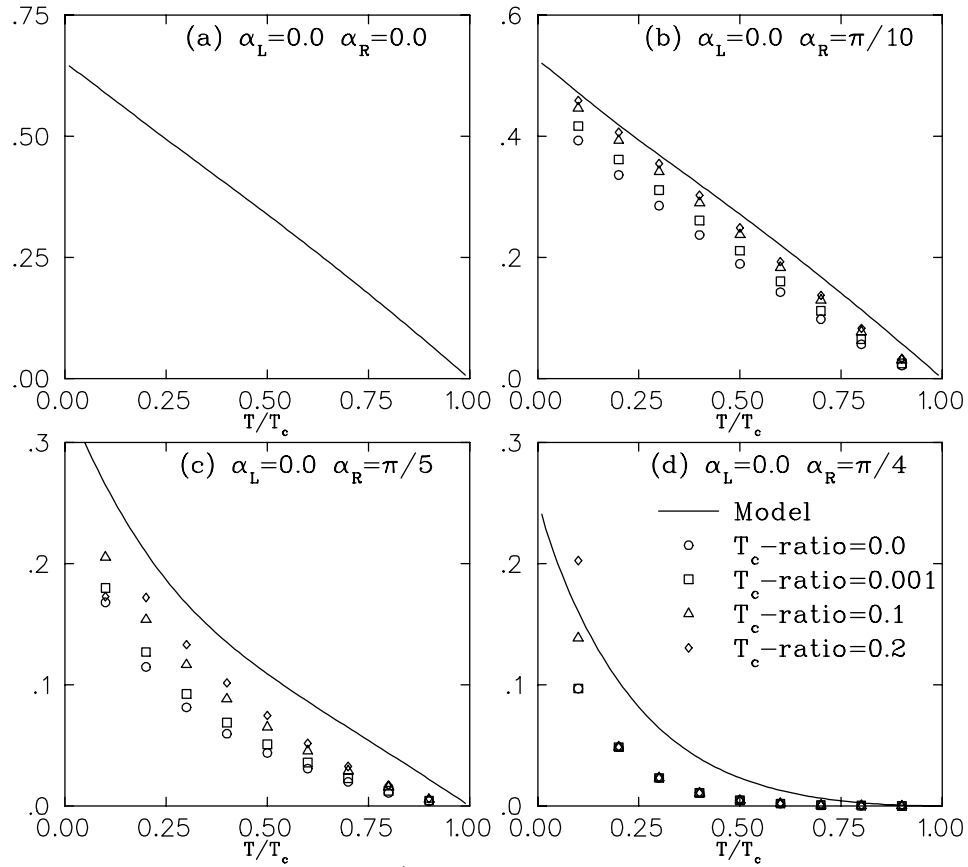


FIG. 4. Critical current vs. temperature in a d-wave/d-wave weak link at four different crystal orientations. Unit of current, $2\pi T_c/R$.

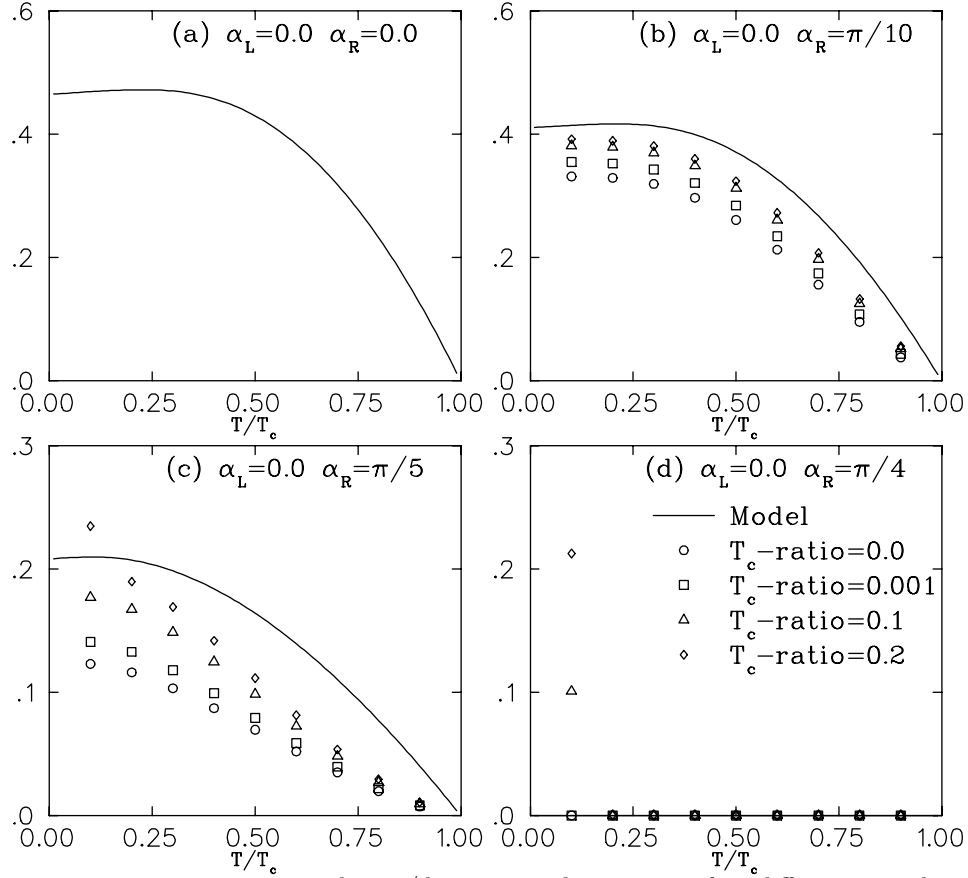


FIG. 5. Critical current vs. temperature in a d-wave/d-wave tunnel junction at four different crystal orientations. Unit of current, $2\pi T_c/R$.

V. CRITICAL CURRENTS AND POSITIONS OF ENERGY MINIMA

A. Critical currents

In Figure 4, the critical current of a weak link between two d-wave superconductors at different crystal misorientations is shown as a function of the temperature. With the misorientation increasing towards $\frac{\pi}{4}$ the temperature dependence of the critical current evolves from linear in $(1 - T/T_c)$ at $\alpha_R = 0$ to quadratic, $(1 - T/T_c)^2$ at $\alpha_R = \frac{\pi}{4}$ for the non-self-consistent (model) calculation and an even higher power for the self-consistent one. The solid line present in Figs.4-6 indicates again (see Section IV A) that the principal effect of the surface scattering is reducing the critical current. Adding a portion of a B_{2g} component compensates for this reduction depending on the relative strengths of the two representations. At misorientations close to $\frac{\pi}{4}$, entering a TRSB state at low temperatures may boost the critical current. Below T_c^{TRSB} the temperature dependence of the critical current undergoes an abrupt deviation from the $(1 - T/T_c)^2$ behavior as clearly seen in Fig. 4(d). In other words, the temperature dependence of the critical current can serve as a detector of a TRSB-state at low temperatures.

In Figure 5 the same temperature dependence as for the weak link in Fig. 4 is shown for a tunnel junction. Same as with the weak link, we see that the critical current is reduced by the surface pair breaking. Approaching $\alpha_R = \frac{\pi}{4}$ extends the initial linear temperature dependence close to T_c to lower temperatures. Right at $\alpha_R = \frac{\pi}{4}$, the current vanishes as long as the superconducting state is not a TRSB-state.

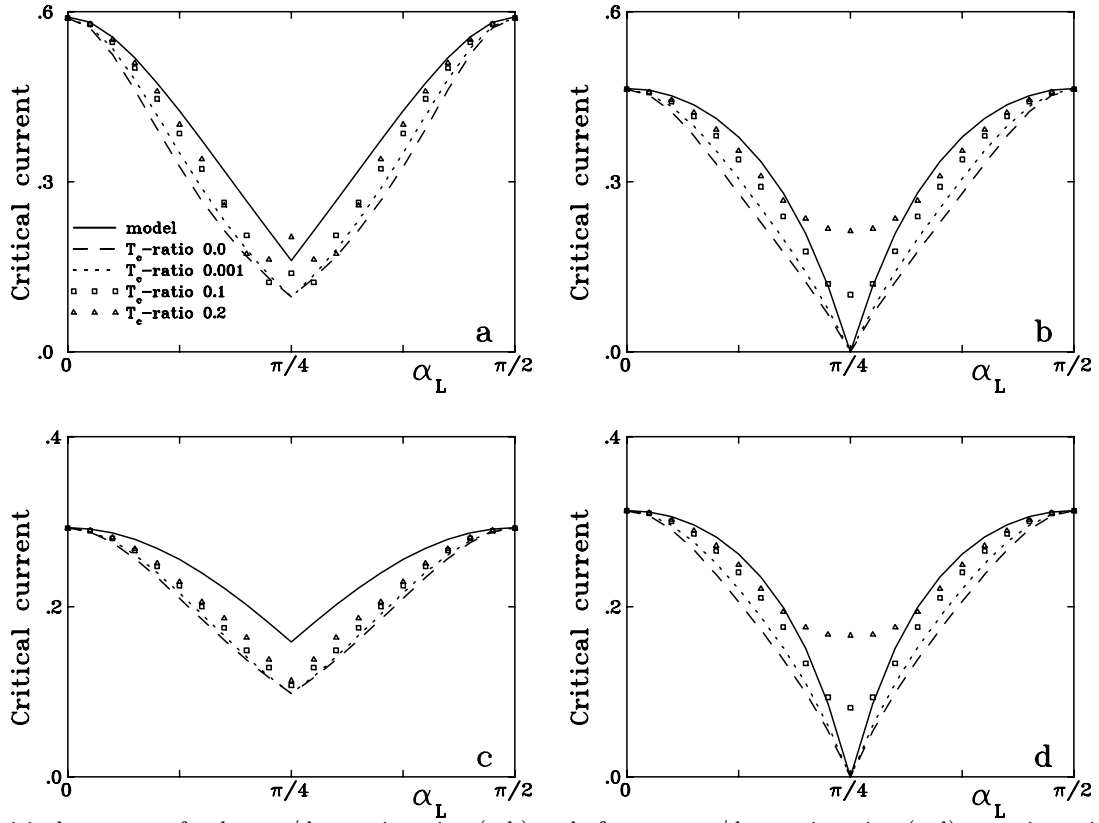


FIG. 6. Critical currents of a d-wave/d-wave junction (a-b) and of an s-wave/d-wave junction (c-d) vs. orientation angle α_L at $T = 0.1T_c$. Weak links, (a),(c); tunnel junctions, (b), (d) .

The critical current at $T = 0.1T_c$ as a function of crystal orientation α_L is shown in Fig. 6. Here $\alpha_R = 0$, i.e, the \hat{a} -axis of one of the superconductors is parallel to the junction normal. In Fig.6 a-b the junction is between two d-wave superconductors and in 6 c-d between a d-wave and an s-wave superconductor. Once more the TRSB-state has a most spectacular effect on the critical current. For the tunneling junction, the critical current no longer vanishes at $\alpha_L = \frac{\pi}{4}$ as in the time-reversal symmetric state.

B. Positions of the energy minima

We now turn to the positions of the energy minima. There is an essential difference between the angular dependences in weak-links and tunnel junctions. If we ignore the change in the order parameter near the surface, the forward (backward) tunneling limit of eq. (10) is

$$j_s(\chi) = j_0 \cos 2\alpha_L \cos 2\alpha_R \sin \chi. \quad (13)$$

This equation was first written down in³⁶, and frequent use of it has been made in the literature (e.g.^{9,8}). It can be rewritten as

$$j_s(\chi) = j_0 \frac{1}{2} (\cos 2\theta + \cos 2(2\alpha_L - \theta)) \sin \chi. \quad (14)$$

with $\theta = \alpha_L - \alpha_R$. Staring at the above (equivalent) equations, one observes that the current-phase relation is sinusoidal which leads to the energy minima of the junction always sitting at the values 0 or π of the phase difference. The rest in the equations can at most change the sign of the current which cannot alter the conclusion that we are always dealing with a normal or a π -junction. As above the phase of the minimum of energy is referred to as χ_{min} . Fig. 7a displays the areas in which χ_{min} takes each of its possible values in terms of the crystal angles. With pure B_{1g} this plot is correct at all temperatures also for the self-consistent solution. It is obvious, as well, that the critical current can only change sign where it vanishes, i.e., when α_L or α_R equals $\pi/4$, $3\pi/4$ etc.

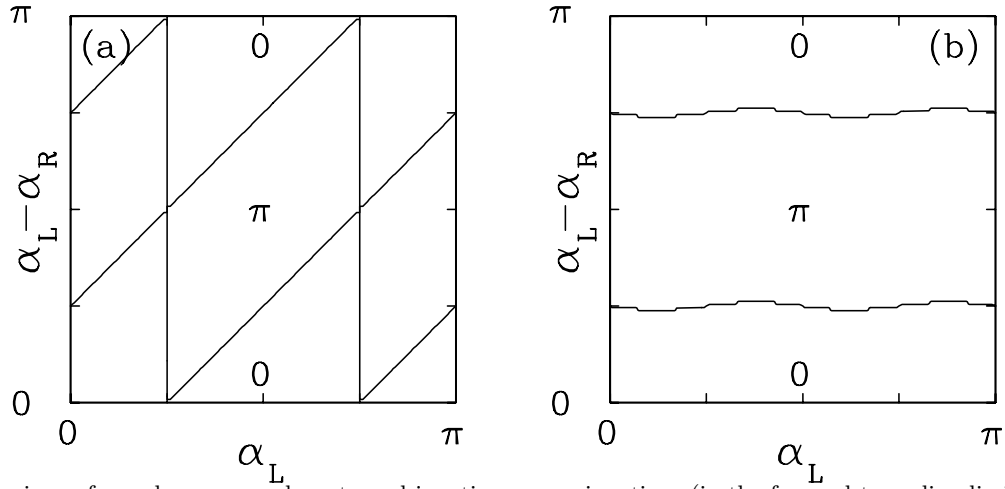


FIG. 7. Comparison of angular ranges where tunnel junctions are π -junctions (in the forward-tunneling limit) between B_{1g} , (a); equation (15), (b).

Now take a look at the pinhole, first at the Ginzburg-Landau limit. At that limit and with a constant $d_{x^2-y^2}$ order parameter up to the junction, equation (8) takes the form

$$j_s(\chi) = j_0(\cos 2\theta - \frac{1}{15} \cos 2(2\alpha_L - \theta)) \sin \chi \quad (15)$$

The argument above that leads to χ_{min} always equal to 0 or π applies here as well. Because of the different coefficients in front of the second cosine terms, Eqs.(14) and (15) deliver very different zones of normal or π behaviors, as highlighted in Fig. 7. Equation (14) assigns the junction orientation an overestimated weight in positioning the π behavior compared to equation (15) which emphasizes the misorientation of the two superconductors. This difference can be ascribed to the pinhole's allowing a larger incident angle for quasiparticles to be transported across the junction. Although illustrated with the non self-consistent order-parameter junction we shall make it clear later that the result is much more general.

Chaudhari and Lin⁸ measured the critical current from a hexagon of $d_{x^2-y^2}$ -superconductor to another crystal of the same superconductor in which the hexagon was inbedded. The misorientation between the two is $\alpha_L - \alpha_R = \frac{\pi}{4}$. The interfaces were the edges of the films which the authors interpreted as tunnel junctions. At the different boundaries of the hexagon the angles α_L were equal to $\frac{\pi}{4}, -\frac{\pi}{12}$ etc. (see Fig. 8) Eq. (14) gives the critical currents across the edges of the hexagon as $j_c = 0, \pm 0.433j_0$. This is in contradiction with the measured currents, which display a modulation around an average current. The result of the experiment has been cited as evidence against the $d_{x^2-y^2}$ -pairing state for the cuprates (see for instance³⁰). Taking the crystal contacts for weak links, the results of Chaudhari and Lin do not rule out the $d_{x^2-y^2}$ -pairing state. In Fig. 9 the critical current at $T = 0.1T_c$ for various T_c -ratios are plotted. The critical current is taken at the constant misorientation $\frac{\pi}{4}$. Picking the simplest case with no subdominant components the critical current oscillates around an average, just as in the experiment. The amplitude of the modulation is admittedly smaller than experimentally reported. Obviously the pinhole is a very idealized model for a weak link, and we cannot expect every small detail getting accounted for.

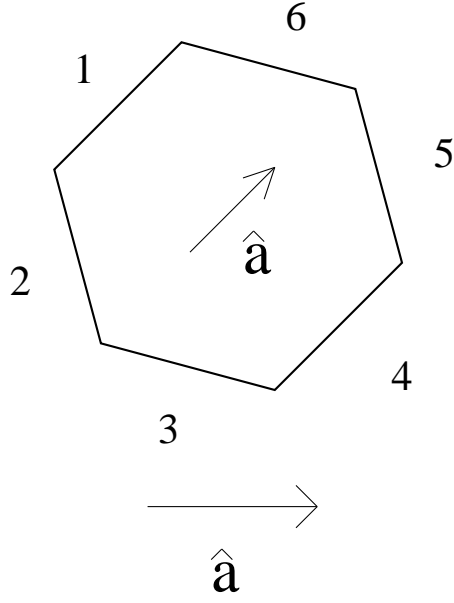


FIG. 8. Hexagonal inclusion of⁸. The inside has the \hat{a} axis rotated through $\pi/4$ with respect to the outside. \hat{a}_{in} is roughly parallel to the sides 1 and 4 in⁸

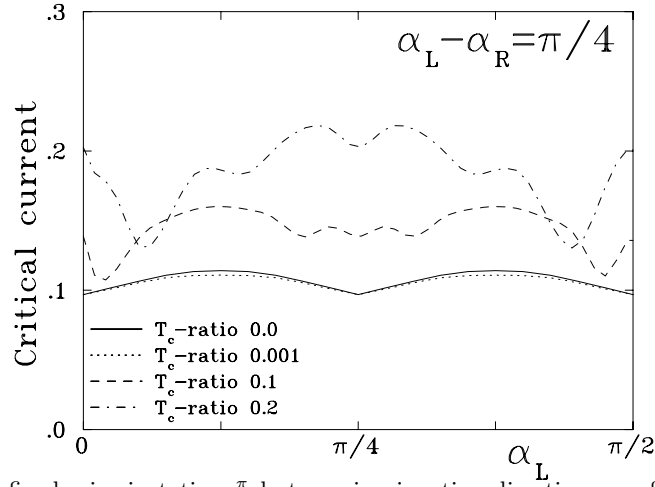


FIG. 9. Critical currents at a fixed misorientation $\frac{\pi}{4}$ but varying junction direction α_L of a weak link at $T = 0.1T_c$. The pattern has the period $\frac{\pi}{2}$.

Away from the Ginzburg-Landau region, the positions of the energy minima were studied numerically. $T = 0.1T_c(B_{1g})$ was chosen. In Figure 10 the position of the energy minima χ_m at a given crystal misorientation and a given junction orientation can be seen for the weak link. The corresponding graphs for the tunnel junction can be found in Fig. 11. For comparison, the junction with a constant order parameter up to the wall without a subdominant component is included. Only one of the two phase differences $(\chi_m^{(1)}, \chi_m^{(2)})$ related through $\chi_m^{(2)} = 2\pi - \chi_m^{(1)}$ is displayed.

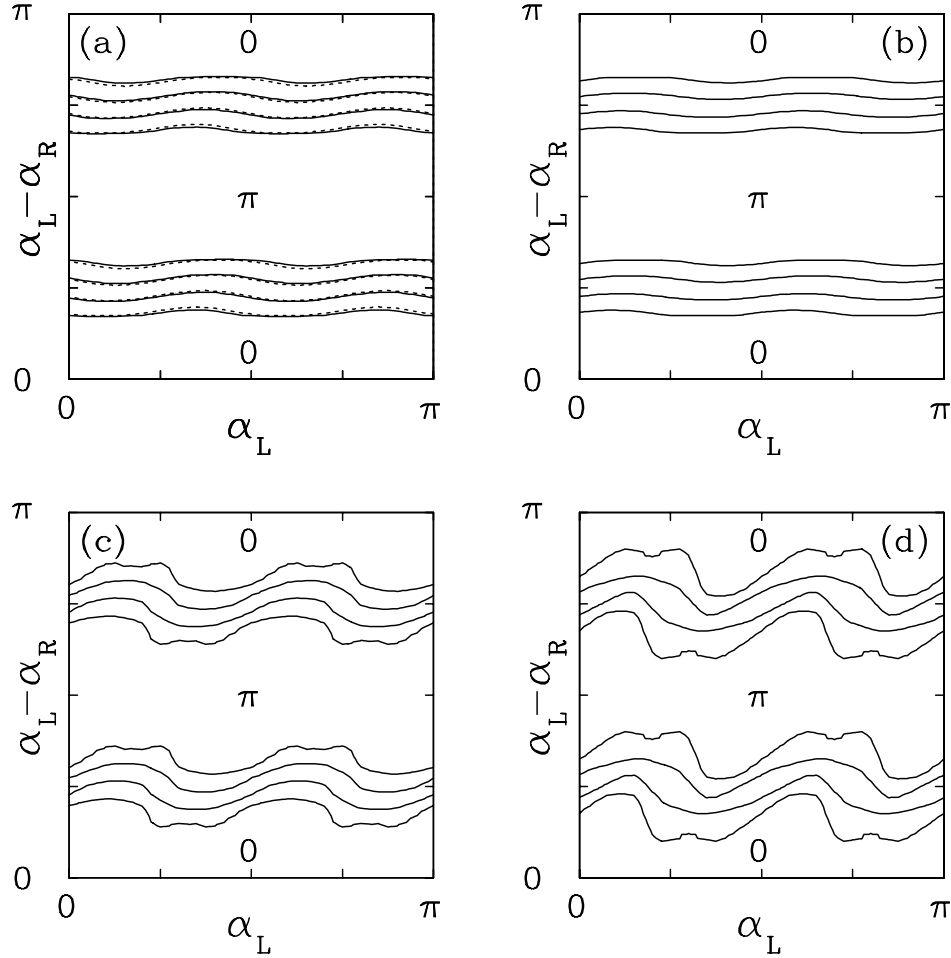


FIG. 10. Contour map of energy minima at $T = 0.1T_c$ in a weak link. Finite slopes are where the junction is neither a 0-junction nor a π -junction. Full lines, self-consistently calculated results, dashed line in (a), constant-order-parameter-up-to-the-wall-model. pure B_{1g} , (a); T_c -ratio 10^{-3} , (b); 0.1, (c); 0.2 (d). With the larger T_c -ratios, the junction orientation acquires an increased importance as the amplitude of the B_{2g} -component depends on the interface orientation.

The constant-order-parameter weak-link junction has zones where χ_m continuously evolves from zero to π . A self-consistently determined order parameter leaves this picture unaltered, i.e. it does not lead to noticeable changes in the positions of the weak-link energy minima at zero T_c -ratio. This is in contrast to the tunnel junction (not in the TRSB-state) where the changes continue being abrupt and the constant-order-parameter model and the self-consistent junction deliver very different pictures (see Fig. 11 a). In the weak link, χ_{min} is a strong function of the misorientation $\alpha_L - \alpha_R$ but depends only weakly on α_L (or α_R) separately. The tunnel-junction χ_m varies as a function of both the misorientation and the junction direction. This is true as long as the admixture of the B_{2g} -component is kept small (in Fig. 10.b T_c -ratio is 10^{-3}). Cranking up the T_c -ratio (see Figs. 10.c-d.) adds structure to the boundary areas between normal and π behaviors of both junction types. Most structure is found when the superconducting state close to the junction breaks time-reversal symmetry with the mixture $d_{x^2+y^2} + id_{xy}$ as the order parameter. The TRSB also smoothes out the jump between the zero junction and the π -junction areas in the tunneling limit.

Higher temperatures only make narrower the zones of continuous change in χ_m from zero to π . Above $0.5 T_c$ this area has essentially vanished and the Ginzburg-Landau formula (15) is an amazingly accurate description of the weak link.

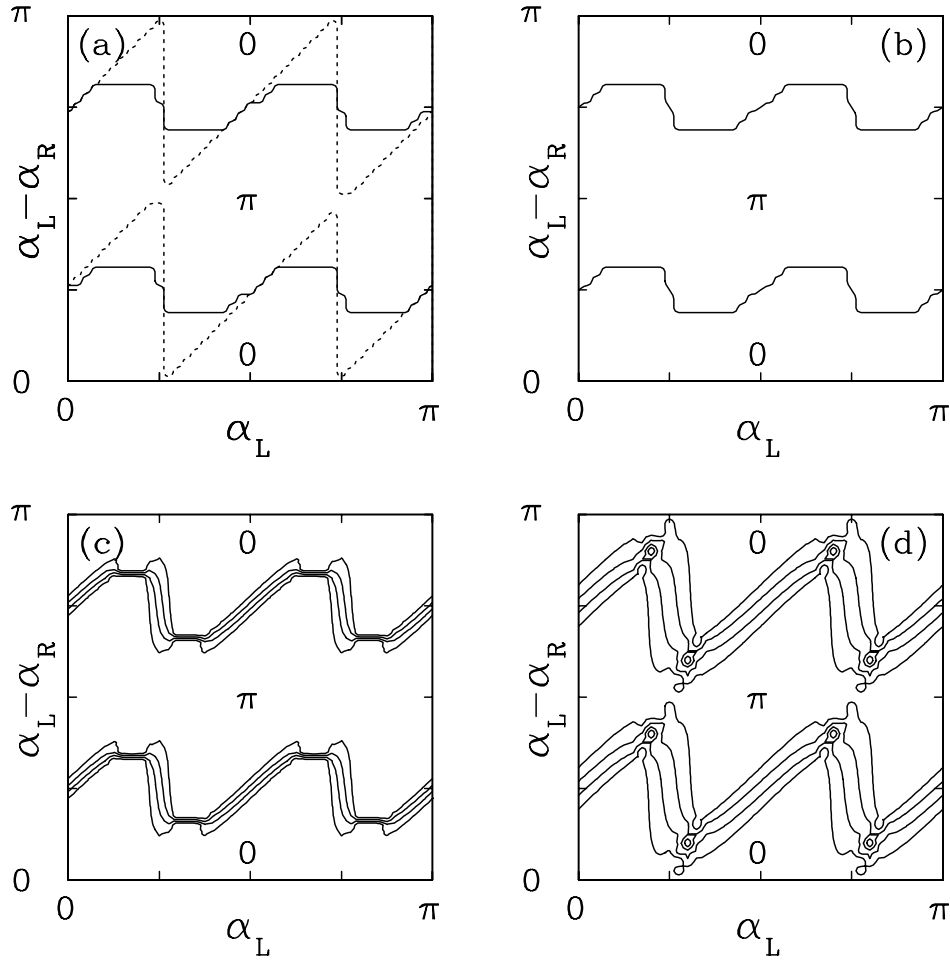


FIG. 11. Contour map of the positions of the energy minima at $T = 0.1T_c$ for a tunnel junction. Full lines indicate self-consistent results, dashed line in (a) constant-order-parameter model. (a) pure B_{1g} superconductors (b) T_c -ratio = 10^{-3} , (c) 0.1, (d) 0.2 (The difference between the full and dashed lines in (a) arises due to the existence of zero energy bound states near the surfaces in those orientations. see^{37,38})

VI. EXPERIMENTAL IMPLICATIONS

A. Small spontaneous fluxes at crystal interfaces

An important implication of the present results bear on the interpretation of the experiment of¹⁰. In this experiment Kirtley et al manufactured triangular or hexagonal inclusions where the region inside was 45 deg misoriented with respect to the outside (similar to that of⁸, see Fig. 8 and Section 5.2). Fluxes spontaneously generated at the corners were measured with a SQUID. The fluxes found were usually small fractions of the flux quantum Φ_0 , neither integer nor half-integer multiples. Moreover, the crystal orientations themselves (with respect to the normal of the junction plane) seem to have no obvious correlation with the fluxes observed (Kirtley, private communication).

When the dimensions of the inclusion for the measurement of flux are much larger than the Josephson penetration length λ_J , the flux generated at a corner should be $\frac{\Phi_0}{2\pi}(\chi_{min}^a - \chi_{min}^b)$ where $\chi_{min}^{a,b}$ are the position of the energy minima of the two interfaces meeting at that corner (see, e.g.³⁹). If one assumes junctions, such as the tunnel junction, which display $\chi_{min} = 0$ or π as long as the order parameter does not break the time reversal symmetry, then the experimental results force one to postulate TRSB at least at the grain boundaries⁴⁰. Even with TRSB, the observation that the crystal orientation themselves seem to have no significant effect on the fluxes observed would still find no explanation. If the bulk order parameter is pure B_{1g} then a TRSB order parameter near the interface can only occur for α_L or α_R near $\pi/4$, whereas $\alpha_R - \alpha_L$ is not directly relevant (c.f. Fig. 7 a.)

If the interfaces are weak-links, however, everything falls in place. Since χ_{min} is neither 0 nor π in general even without TRSB (see Fig. 10). Our unit-transmission limit seems to be somewhat too extreme, however, in that χ_{min}

depends on $\alpha_L - \alpha_R$ but is almost independent on the individual α_L or α_R . For pure B_{1g} , the theoretical fluxes are too small. This holds true also with a substantial B_{2g} component induced near the grain boundaries as long as we are not in a TRSB state (see Fig. 10). In reality the grain boundary is more likely to have a smaller than unity transmission coefficient, so that χ_{min} would vary stronger with the α 's (i.e, with pure B_{1g} , the portrait of χ_{min} would have to evolve from Fig. 10 a to Fig. 7 a when the transmission decreases).⁶

The condition $\alpha_L - \alpha_R$ approximately equal to $\pi/4$ is crucial. For example other experiments involving misoriented crystals,^{9,12,13} (as well as the "frustrated" samples of⁷) all have misorientations close to (but sometimes not exactly) $\pi/6$ and one of the α 's is approximately zero. (or those related to these by symmetry) Our pinhole results for χ_{min} with the transmission coefficient equal to unity, differ only very slightly from the corresponding tunnel-junction values. (For the junctions with $\alpha_L = 0, \alpha_R = \pm\pi/6$, $\chi_{min} \approx 0.17\pi$ ⁷ rather than $\chi_m = 0$ for tunnel junctions without broken time reversal symmetry.). The deviation for these new energy minima will be even smaller with a smaller transmission coefficient and/or more directional tunneling. Thus our picture for the small spontaneously fluxes of¹⁰ is not inconsistent with all these experiments. It would be interesting experimentally to try to observe the fluxes, if any, that nucleate at the corners of the inclusions with misorientation of $\pi/6$ with judicious choice of α 's. Obviously the results expected from the energy minima based on weak-links (Fig 10) will be very different from those based on eq(13) (Fig 7 a) as well as those from tunnel junctions with TRSB near the interfaces (Fig 11 c,d).

B. The transmission coefficient of a junction

J_c across grain boundaries have been measured. They range from $\sim 10^3 A/cm^2$ to $\sim 10^5 A/cm^2$ for $T \ll T_c$ (e.g.^{7, 89, 12, 13}). A transmission coefficient can be inferred from these values. The critical current for a weak-link is dictated by the formation of phase slip centers and is not equal to the thermodynamic current directly related to the transmission coefficient. Recently¹² and¹³ have reported direct measurements of the Josephson penetration depth λ_J via the observation of fluxes along the grain boundaries and the corner of the tricrystals (with a misorientation of ~ 30 deg). We shall try to estimate the transmission probability $|T|^2$ from their λ_J . With $\lambda_J^{-2} = \frac{8\pi J_c}{\hbar c^2} w$ where w is the thickness of the magnetic field penetration layer along the barrier, and with the rough formula $J_c \sim \pi \Delta N_f v_f e |T|^2$ for the critical current density, as well as $\lambda_L^{-2} = 4\pi N_f v_f^2 e^2 / c$ for the London penetration length, we arrive at $\frac{\lambda_J^2}{\lambda_L^2} \sim \frac{w}{\xi_0} |T|^2$ where $\xi_0 = \frac{\hbar v_f}{\pi \Delta}$ is the zero temperature coherence length. For $YBCO$, if we take $\lambda_L \approx 1400 \text{ \AA}$, $\xi_0 \approx 14 \text{ \AA}$, with $\lambda_J \sim \mu m$ and $w \approx 2\lambda_L$, we get $|T|^2 \sim 10^{-4}$. Estimates for $TlBaCuO$ are similar. At first sight then, $|T|^2$ seems small enough in the 30 deg misoriented films for one to assume the tunneling limit. If we accept the same order of magnitude for $|T|^2$ in¹⁰, then our scenario for the new χ_m seem not very plausible. One needs to keep in mind, however, that the estimate is an average transmission coefficient. Electrical conduction may proceed through "hot spots" of much higher transparency. If we take the extreme limit of the pinholes with unit transmission, then the fraction of transparent area is $\approx 10^{-4}$. It is possible that the non-uniformity of the critical current densities cannot be seen in the scanning SQUID measurements if the distances between the pinholes are $\ll \lambda_J$. If d is the average pinhole-pinhole distance and $(a/d)^2 \sim 10^{-4}$, there remains reasonable margin for the parameters a and d even with the restriction $a \ll \xi_0 \ll d \ll \lambda_J$ for our calculation to apply. In¹⁰, the authors themselves emphasized that the fluxes would be much more localized than expected if λ_J were $\sim \mu m$, which may suggest that the boundaries are very non-uniform.

VII. CONCLUSION

In conclusion we have investigated the difference between high and low transmission junction in d-wave superconductors, using pinhole as an extreme example in the high transmission limit. The effects of subdominant order parameter were also considered.

Acknowledgement

This research was supported in part by the NSF through the Northwestern University Materials Research Center, grant no. DMR 91-20521 (SY), the Science and Technology Center for Superconductivity, grant no. DMR 91-20000

⁶Details of the calculations with a finite transmission coefficient will be reported separately

⁷ this value is for at $T/T_c = 0.1$, slightly higher than that appropriate for some of the experiments ($T \approx 4.2K$, $T_c \approx 90K$).

(MF and SY), and Academy of Finland under contract No. 1081066 (MF) and on a sabbatical leave (JK). MF also acknowledges partial support from SFÄAF, Åbo Akademi and Magnus Ehrnrooths Stiftelse. Two of us (JK and SY) would like to thank Aspen Center for Physics, where this collaboration was initiated.

- ¹ Scalapino D.: *Phys. Rep.* 250, 329 (1995)
- ² Annett J., Goldenfeld N. and Leggett A. J.: *preprint*: cond-mat/9601060, (1996)
- ³ Wollman D. A. et al: *Phys. Rev. Lett.* 71, 2134 (1993)
- ⁴ Brawner D. A. and Ott H. R.: *Phys. Rev. B* 50, 6530 (1994)
- ⁵ Iguchi I. and Wen Z.: *Phys. Rev. B* 49, 12388 (1994)
- ⁶ Wollman D. A. et al: *Phys. Rev. Lett.* 74, 797 (1995)
- ⁷ Miller Jr. J. H., et al: *Phys. Rev. Lett.* 74, 2347 (1995)
- ⁸ Chaudhari P. and Lin S-Y.: *Phys. Rev. Lett.* 72, 1084 (1994)
- ⁹ Tsuei C. C., et al: *Phys. Rev. Lett.* 73, 593 (1994)
- ¹⁰ Kirtley J. et al: *Phys. Rev. B* 51, 12057 (1995)
- ¹¹ Mathai A. et al : *Phys. Rev. Lett* 74, 4523 (1995)
- ¹² Tsuei C. C., et al: *Science* 271, 329 (1996)
- ¹³ Kirtley J. et al: *Phys. Rev. Lett.* 76, 1336 (1996)
- ¹⁴ Likharev K. K.: *Rev. Mod. Phys.* 51, 101 (1979)
- ¹⁵ Yip S.: *Phys. Rev. B* 52, 3087 (1995)
- ¹⁶ Barash Yu. S. Galaktionov A. V. and Zaikin A. D.: *Phys. Rev. B* 52, 665 (1995)
- ¹⁷ Ambegaokar V., deGennes P.G and Rainer D.: *Phys. Rev. A* 9, 2676 (1974)
- ¹⁸ Buchholtz L., Palumbo M., Rainer D. and Sauls J. A.: *J. Low Temp. Phys.* 101, 1079 (1995); *ibid* 101, 1099 (1995)
- ¹⁹ Mannhart J. et al , *Phys. Rev. Lett* 77, 2782 (1996)
- ²⁰ Kulik I. O. and Omel'yanchuk A. N.: *Fiz. Nizk. Temp.* 3, 945 (1977)
- ²¹ Kopnin N. B.: *JETP Lett.* 43, 708 (1986)
- ²² Kurkijärvi J.: *Phys. Rev. B* 38, 11184 (1988)
- ²³ Kurkijärvi J, Rainer D and Sauls J. A.: *Can. J. Phys.* 65, 1440 (1987)
- ²⁴ Fogelström M, Kurkijärvi J. and Sauls J. A.: Proceedings of the First International Conference on Quasiclassical Methods in Superconductivity and Superfluidity, Verditz, Austria.
- ²⁵ Matsumoto M., and Shiba H.: *J. Phys. Soc. Japan* 64, 1703 (1995); *ibid* 64, 3384 (1995); *ibid* 64, 4867 (1995)
- ²⁶ Zhang W.: *Phys. Rev. B* 52, 3772 (1995), *Phys. Rev. B* 52, 12538 (1995)
- ²⁷ Fogelström M., Rainer D. and Sauls J. A.: *Phys. Rev. Lett.* 79, 281 (1997); Fogelström M., Palumbo M., Buchholtz L. J., Rainer D. and Sauls J. A.: *preprint*
- ²⁸ Serene J. W., and Rainer D.: *Physics Reports* 101, 221 (1983)
- ²⁹ Palumbo M., Buchholtz L., Rainer D. and Sauls J. A.: Proceedings of the First International Conference on Quasiclassical Methods in Superconductivity and Superfluidity, Verditz, Austria.
- ³⁰ Sigrist M, and Rice T.M.: *Rev. Mod. Phys.* 67, 503 (1995)
- ³¹ Thuneberg E. V., Kurkijärvi J. and Rainer D.: *Phys. Rev. B* 29, 3913 (1984)
- ³² Radtke R. J., Ullah S., Levin K., and Norman M. R. *Phys. Rev. B* 46, 11975 (1992)
- ³³ Millis A. J., Rainer D. and Sauls J. A.: *Phys. Rev. B.* 38, 4504 (1988)
- ³⁴ Yip S.: *J. Low Temp. Phys.* 91 203 (1993)
- ³⁵ Ambegaokar V. and Baratoff A.: *Phys. Rev. Lett.* 10, 486 (1963).
- ³⁶ Sigrist M, and Rice T.M.: *J. Phys. Soc. Japan* 61, 4283 (1992)
- ³⁷ Tanaka Y. and Kashiwaya S., *Phys. Rev.* B53, 11957 (1996)
- ³⁸ Barash Yu S., Burkhardt H. and Rainer D., *Phys. Rev. Lett.* 77, 4070 (1996)
- ³⁹ Millis A. J.: *Phys. Rev. B* 49, 15408 (1994)
- ⁴⁰ Sigrist M, Bailey D. B. and Laughlin R. B.: *Phys. Rev. Lett.* 74, 3249 (1995)